Metal-insulator transition in doped polymerized polyaniline

R. A. Padilla,[1,*] M. A. Pacheco,[1] and E. V. Anda[2]

[1]*Departamento de Engenharia Elétrica, Pontifícia Universidade Católica do Rio de Janeiro (PUC-Rio), Rio de Janeiro 22451-900, Brazil*

[2]*Departamento de Física, Pontifícia Universidade Católica do Rio de Janeiro (PUC-Rio), Rio de Janeiro 22451-900, Brazil*

(Received 14 March 2019; revised manuscript received 27 August 2019; published 10 September 2019)

In this paper, the metal-insulator transition is studied in polyaniline (PANI) as the doping increases. The study incorporates a polymerization process that produces a cross-linking of the PANI chains, yielding an extended disordered branched lattice. The presence of the phenazine structure is fundamental and allows the polymer to acquire extra dimensions, which permits a transition to the metallic phase when doping is increased as the Fermi level goes through the mobility edge into a region of extended states. This PANI system is described assuming that the polymerization process gives rise to a structure that could be represented by a Bethe lattice. It is observed, as indicated by the experiments, that the conductivity increases as a function of the pH of the acid solution when agents like bipolarons are introduced.

DOI: 10.1103/PhysRevB.100.115116

I. INTRODUCTION

There is significant interest in studying conjugated organic polymers due to their metallic properties when they are highly doped. The flexibility to change their conductivity has opened the possibility for various applications, representing an alternative to traditional conducting materials. Polyaniline (PANI) is considered the most promising material due to its excellent stability, high conductivity, and excellent optical properties [1,2]. The growing interest in nanostructured conducting PANI is due to its use in the construction of new electronic devices such as transistors [3], supercapacitors [4], and energy storage cells [5]. Many synthesized forms of nanostructure PANI are obtained at an early stage, during the polymerization of aniline in acidic solutions. The growth mechanism and the exact nanoscale molecular structures formed in the polymerization process are still controversial [6–12].

In recent years, progress has been achieved [13–16] with regard to the structural characterization of aniline oligomers formed during the oxidative polymerization in solutions of pH from 2.5 to 10. The polymerization process has essential consequences in conductance, as it gives rise to the formation of disordered lattice structures [17,18] with effective dimension greater than 1. The dimension, in turn, is of fundamental importance for the appearance of delocalized states participating in the charge transport. The electrical conductivity results from the existence of charge carriers, which are introduced by doping and move along the conjugated π bonds. In the different composition forms of PANI, the emeraldine base form EB-PANI (insulator) is more stable and it is the one which becomes conductive when doped by reacting with a strong acid (e.g., HCl), resulting in the conductive emeraldine salt form ES-PANI [19,20].

One debatable topic in the literature refers to the formation of doped PANI. Several authors have investigated the electronic structure in a disordered one-dimensional PANI chain using molecular orbital calculations [21,22]. Some authors consider the bipolaron lattice [23–26] a suitable candidate, being the final state of PANI and, upon protonation, highly conductive. The polaronic model for conduction in fully protonated ES-PANI is also theoretically supported by some proposals [27–29]. In a more recent work [30], we proved that bipolaron polaron doped disordered long chains of PANI, in the limit of zero inelastic scattering, possess zero conductance because of Anderson localization [31]. This showed that the description of disordered polymerized PANI as a linear one-dimensional model does not manifest correlated disorder and delocalization at the Fermi level as has been proposed [23–26,28]. The lack of charge diffusion at the Fermi energy indicates that this one-dimensional description of the system is not adequate. Although experimental and theoretical studies emphasize the importance of interchain interactions, as well as the three-dimensionality nature of the electronic states in highly conductive polymers [32–36], recent works [23,24] have continued treating polyaniline as a linear chain model.

In this paper, we propose a model to study the transport properties of the PANI polymer where, in contrast to the one-dimensional model, an analysis of the PANI lattice formation in the oxidative polymerization of aniline is incorporated to understand the evolution of the molecular structure. Growing chains are simultaneously organized as complex supramolecules [17,18,37], leading to the formation of cross-links that yield the PANI's nanostructures. The mechanism of oxidative polymerization has been studied by semiempirical quantum chemical methods and it was revealed that, depending on the pH of the reaction medium, various molecular (branched vs linear) oligomeric structures are formed [6–8,38], showing that the proportion of the structures increases with increasing acidity [7]. As the component that produces the cross-linking of the lattice, the phenazine [39–43] molecule plays a vital role in the structural characteristics of PANI, being responsible for the resulting

*ar1pa@hotmail.com

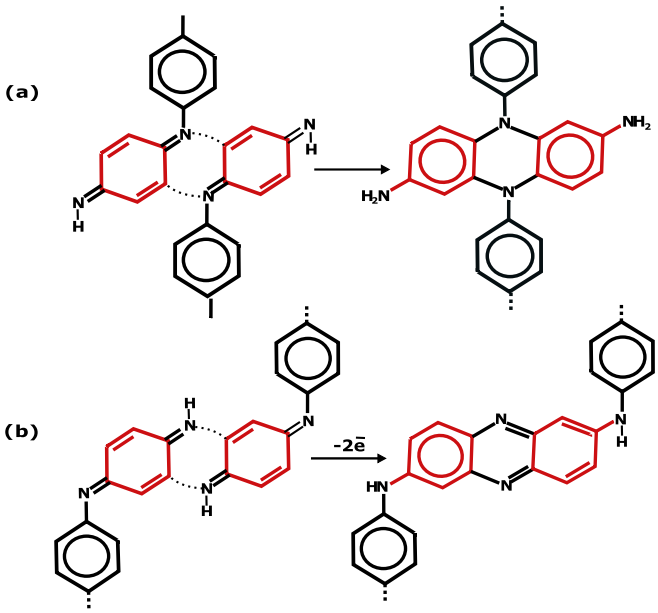

FIG. 1. Two proposed formation mechanisms of intermediate tetramerlike phenazine [53], where the cross-linking branched chains of PANI occur.

supramolecular morphology of the conductive PANI. A variety of intermediate aggregates, formed at the early stage of aniline chemical oxidative polymerization, is described in the literature [17,18,37,44]. Structures like "phenazine" are found in the doped form of PANI [45–52] and are considered in this work as the fundamental core for building extensive cross-linked chains of PANI.

Based on characterization results, several authors [8,44,53] proposed the tetramer oligomer as the component of the intermediate aggregates containing the symmetric phenazine and the dihydrophenazine structures. These symmetric planar aggregates led to strong π-π interactions, which serve as supporting evidence for the proposed formation mechanism. It has been suggested [53] that these tetramers have two major geometries, as shown in Figs. 1(a) and 1(b), involving at least two plausible cross-linking routes for the formation of tetramer structures. The proposed reaction mechanism explains the pathways for the creation of intermediate tetramers, formed by cross-linking between oxidized dimers. Based on this evidence, we consider the phenazine tetramer structure in Fig. 1(a) as the better choice for the central core to build a realistic extensive and disordered branched PANI structure, which is modeled by a Bethe lattice (BL) as detailed in Sec. II.

In this paper, we study the metal-insulator transition in the cross-linked branched PANI polymer, including the disorder distribution of bipolarons [21,25] (random along the chains) and the degree of doping [54–58], usually depending on the protonation rate within the PANI system. A branched lattice system is constructed taking the phenazine molecule as the nucleus, which produces the ramification of the extensive and disorderly branched PANI lattice. This allows for a more reliable reproduction of a real nanostructure of PANI, avoiding the one-dimensional disordered lattice description that gives rise to unrealistic Anderson localized states at the Fermi energy [31]. We theoretically analyzed its existing transport properties and compared it with the experimental results. In Sec. III, we describe the system represented by the tight-binding Hamiltonian [28,59] within the Hückel model [21,22,29,60]. The Green's function methodology and its nonequilibrium Keldysh formulation [61,62] were used to obtain the local density of states (LDOS) and the conductance [63]. The results are discussed in Sec. IV. Our theoretical predictions ae compared with the experimental results [19,20,64–69] of the conductance as a function of the pH in the aqueous solution.

II. BETHE LATTICE MODEL

The Bethe lattice model can be used to study the electronic structure in ordered and disordered systems [70–73]. The BL model may be defined as an infinite tree, admitting an exact solution and reflecting essential features in one-body interacting systems [74]. Systems involving interactions and, in particular, disorder can be solved satisfactorily in a BL context [74–78] and we utilize it to study the disordered branched structure of PANI.

A structure similar to a BL has been proposed to study the effect of disorder on the transport properties of polymers [36]. This toy model was capable of predicting, in a qualitative way, a metal-nonmetal transition, reflecting the well-known proprieties of a disordered BL [79]. However, this result does not sustain a real experimental comparison, due to the simplicity of the model. The one-dimensional description of PANI, although incapable of describing the transport properties of polymers, is still thought to be an adequate model for study of these systems [23,24]. Due to this situation, it is very important to adopt a reliable and realistic framework to analyze them. Our proposal permits the development of a detailed analysis of the physics associated with the disorder in polymers, describing the appearance of mobility edges, separated in energy localized from extended states. A one-body interacting system, defined on a disordered BL, allows a numerical solution where these properties can be studied in a reliable and almost-exact way [78].

Following these ideas, we graphically represent in Fig. 2 the lattices used to model the disordered branched PANI. A simple finite linear PANI can be constructed by a sequence of m and M structures, each one with three possible configurations, as shown in the figure. The figure also includes the phenazine representation, according to its molecular configuration [Fig. 1(a)], which plays a fundamental role in the construction of the BL. Phenazine (P) can also be doped by changing the local energy of the protonated site (P^+). These representations are sufficient to generate the EB-PANI (unprotonated) as well as the protonated ES-PANI form.

Finally, a branched PANI is an infinite connected lattice where each node, represented by a phenazine structure P (P^+), possesses the vertices α, β, γ and δ, through which it is connected to $Z = 4$ neighbors, where Z is the coordination number of the lattice. We construct a sample of BL-PANI in the following way.

i. A simple finite linear PANI can be constructed by a sequence $-m - M - \cdots - m - M-$. In this conformation, m and M are chosen at random from their three possible structure representations, as presented in Fig. 2, where the lattices

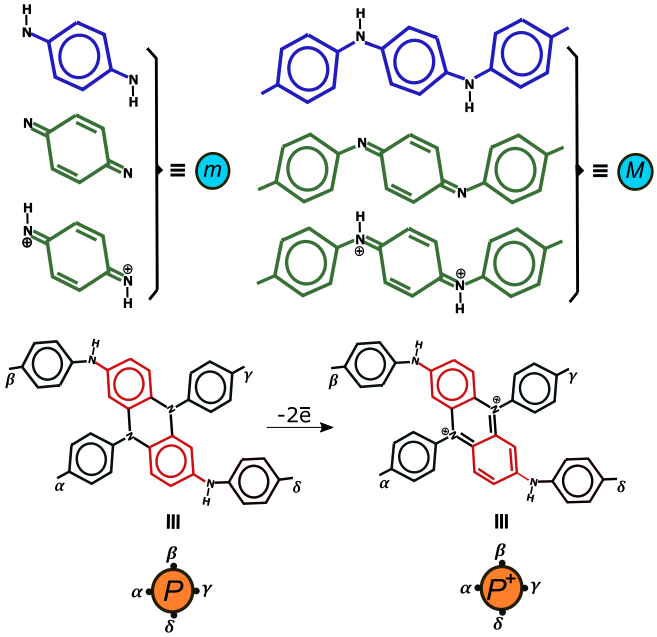

FIG. 2. Structures that compose the BL, $Z = 4$, model of a branched cross-linking PANI. P and P^+ represent nondoped and doped phenazine, respectively, and their corresponding sites inside the structure.

containing the structure (-⊕NH-) are chosen in a percentage compatible with the doping concentration.

ii. We randomly select Z PANI chains from a set of 20, constructed with different lengths, formed by 10 to 50 m and M structures (Fig. 2). This gives rise to finite ordered and disordered chains for undoped/doped forms of PANI.

iii. In the initial stage of the branched process, $Z - 1$ of these linear PANI samples are connected to its adjacent semi-infinite lead, representing the contacts, through the hopping matrix element t as depicted in Fig. 3.

iv. In the next stages, three of the red cluster BL-PANI represented in Fig. 3 are used as new contacts at sites i', i'', and i''' connected by a hopping parameter t'. Using the self-similarity property of the BL, we recursively apply this procedure to construct the final and complete PANI structure.

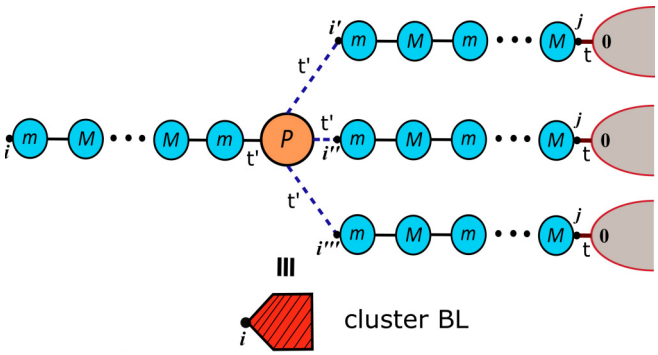

FIG. 3. BL model in the initial stage of the branched PANI system with coordination number $Z = 4$. At $Z = 4$, the central core phenazine represented by P is connected to the left with 1 and to the right with $Z - 1$ PANI linear chains by the hopping parameter t'. The complex structure at site i is represented by the red cluster.

Thus, the first BL cluster is constructed by connecting the site of the nearest neighbor in each linear chain with the specific sites (α, β, γ, and δ) of the phenazine molecule. As previously mentioned, in the next d steps, the previous BL clusters formed with $Z = 4$ may be used recursively to generate a more extensive BL, reaching a number of total sites that increase exponentially (with the number d) of the order of 10^6 sites. In this way, the BL model can represent a more realistic nanostructured PANI having branches by means of a cross-linking procedure. This allows the simulation of a very extensive disordered BL-PANI sample without significant computational effort [73].

III. GREEN'S FUNCTIONS AND CONDUCTANCE

The linear chain sample and the phenazine molecules used to build the BL-PANI system are modeled by a discrete level tight-binding Hamiltonian [28,59] written as

$$H = \sum_{i=1}^{N} \epsilon_i n_i + \sum_{i,j>i}^{N} V_{ij}(c_i^\dagger c_j + \text{H.c.}), \tag{1}$$

where the first term describes site i with energy ε_i, $n_i = c_i^\dagger c_i$ is the number operator, the fermionic operator $c_i^\dagger$ (c_i) creates (annihilates) an electron at site i, and V_{ij} is a potential hopping matrix element between state $|i\rangle$ and state $|j\rangle$, which is considered to be nonzero only for nearest-neighbor sites. In order to represent the proprieties of a real PANI lattice, the matrix elements of the Hamiltonian are obtained from Huckel theory by using the Streitwieser parameters [60].

We exactly diagonalize the tight-binding Hamiltonian to obtain their eigenvalues and eigenvectors. To study the dynamics of the system, we calculate the equilibrium Green's function [61,80] for the first linear chain (Fig. 3) connected to the phenazine P. This lattice is defined from site i to sites at the phenazine itself, β, γ, and δ (Fig. 2). The Green's functions used to construct the whole PANI lattice, as discussed in the Appendix, are given by

$$g_{rs}(w) = \sum_{\lambda} \frac{a_\lambda(r) a_\lambda^*(s)}{w - \varepsilon_\lambda + i\eta}, \tag{2}$$

where ε_λ represents the Hamiltonian eigenvalues such that $H|\psi_\lambda\rangle = \varepsilon_\lambda|\psi_\lambda\rangle$ and the eigenvector $|\psi_\lambda\rangle$ is given by $|\psi_\lambda\rangle = \sum a_\lambda(r)|\varphi_r\rangle$, and $|\varphi_r\rangle$ is the atomic wave function at site r used to obtain the Hamiltonian in the tight-binding representation. As usual, an infinitesimal imaginary quantity η is defined at the denominator of Eq. (2) to regularize the Green's function at the real axis. Calculating $g_{rs}(w)$ using Eq. (2), we can get the dynamical properties as the conductance through nonequilibrium Green's function formalism [61,62] as shown in the Appendix. In a system composed of two extended BL-PANI, as described in Fig. 4, we obtain the current [63,81] going along site 0 by

$$J_{\text{curr}} = \frac{2e^2}{h} \int_{-\infty}^{\infty} T(\varepsilon)[f(\varepsilon - \mu_L) - f(\varepsilon - \mu_R)]d\varepsilon, \tag{3}$$

where $T(\varepsilon)$ is the transmission, $f(\varepsilon)$ the Fermi Dirac distribution, and $\mu_{L,R}$ the Fermi energy of the left and right reservoirs, respectively. In the case of an infinitesimal bias potential, from Eq. (3), one obtains the familiar expression for

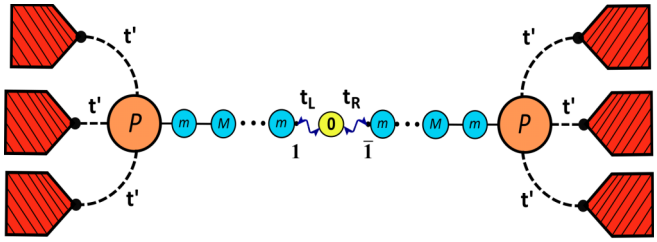

FIG. 4. Total system of two extended branched BL-PANIs with coordination number $Z = 4$, where the conductance is obtained calculating the current going along site 0.

the conductance $G = \frac{2e^2}{h}T(\varepsilon_f)$, with the transmission at the Fermi level, given by

$$T(\varepsilon_f) = 4\pi^2 t_L^2 t_R^2 \rho_1(\varepsilon_f)\rho_{\bar{1}}(\varepsilon_f)|G_{00}(\varepsilon_f)|^2, \tag{4}$$

where the quantum unit of conductance $2e^2/h = 77.5 \times 10^{-6}\ \Omega^{-1}$ or S (Siemens). In this equation $\rho_1(w)$ and $\rho_{\bar{1}}(w)$ are the LDOS values of the semi-infinite BL-PANI at sites 1 and $\bar{1}$, as indicated in Fig. 4, and G_{00} is the diagonal Green's function at site 0 of the complete lattice, shown in Fig. 4. Green's functions are calculated using Dyson's equation, as discussed in detail in the Appendix. Each cluster BL represents an extensive random BL-PANI connected through its respective hopping parameter t_L or t_R (left and right). The Green's function, $G_{00}(\varepsilon_f)$, with local energy ε_0 corresponding to the first site of (-NH-), (-N=), or (-⊕NH-), in the different conformations of the m structure, as shown in Fig. 2, is given by

$$G_{00}(\varepsilon) = \frac{1}{w - \varepsilon_\alpha + i\eta - g_{11}(\varepsilon)t_L^2 - g_{\bar{1}\bar{1}}(\varepsilon)t_R^2}. \tag{5}$$

To obtain the conductance, as mentioned before, we construct a BL through a process of d steps, thereby achieving a large number of sites to model the BL-PANI system. This permits a good statistical treatment of the disorder introduced by doping to study the physical properties involved.

IV. RESULTS

The charge transport properties of PANI are studied analyzing its conductance as a function of the doping. The relationship of doping produced by protonation with the pH of the aqueous solution allows comparison of our results with experiments. The concentration (%) of doping as a function of the pH of the aqueous solution can be obtained using a statistical mechanics framework [82–84] and is given by

$$\frac{\langle n\rangle}{\langle N\rangle} = \frac{\kappa e^{-2.303\text{pH}}}{1/2 + 2\kappa e^{-2.303\text{pH}} + (1/4 + \kappa e^{-2.303\text{pH}})^{1/2}}, \tag{6}$$

where $\frac{\langle n\rangle}{\langle N\rangle}$ is the fraction of nitrogen atoms with absorbed protons, which proves to be the percentage doping. In this equation, $\langle n\rangle$ is the number of (-⊕NH-) structures and $\langle N\rangle$ the total number of nitrogens. The constant involved, $\kappa = 34.03$, is determined by fitting the equation to the experimental data [82,83]. This relationship, depicted in Fig. 5, allows

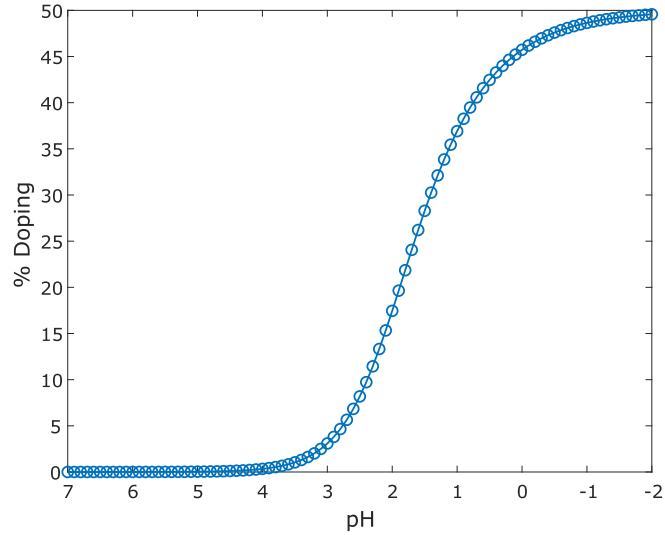

FIG. 5. Behavior of the doping percentage dependence of EB-PANI as a function of the pH of the HCl solution.

the study of the metal-insulator transition in branched PANI systems as a function of the pH.

In all the results, we simulate a set of random BL-PANI samples (extension $d = 6$) where the conductance and LDOS are calculated considering a spatial average of 55 total configurations. Henceforth, the entire energy range ω, with an interval of 10^{-6} between each energy, is measured in units of β, the carbon-carbon ligand energy ($\beta \approx 2.5$ eV [60]).

Initially, we analyze the case when the system is not doped, so that the linear chains and the phenazine that yield the BL are not protonated. In Fig. 6 we show the LDOS and the conductance for the ordered EB-PANI and zero doping. The Fermi level is located in the gap region, corroborating that this system is an insulator.

For the case of protonated PANI, we construct disordered linear chains, randomly distributing pairs of (-⊕NH=) creating groups of bipolarons. The phenazine can be chosen

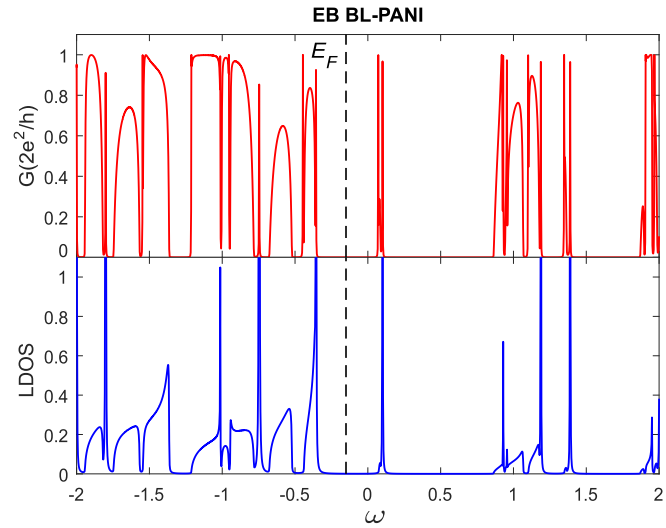

FIG. 6. Conductance and LDOS for an ordered EB-PANI showing the Fermi level (dashed line) for a BL of 40×10^6 sites.

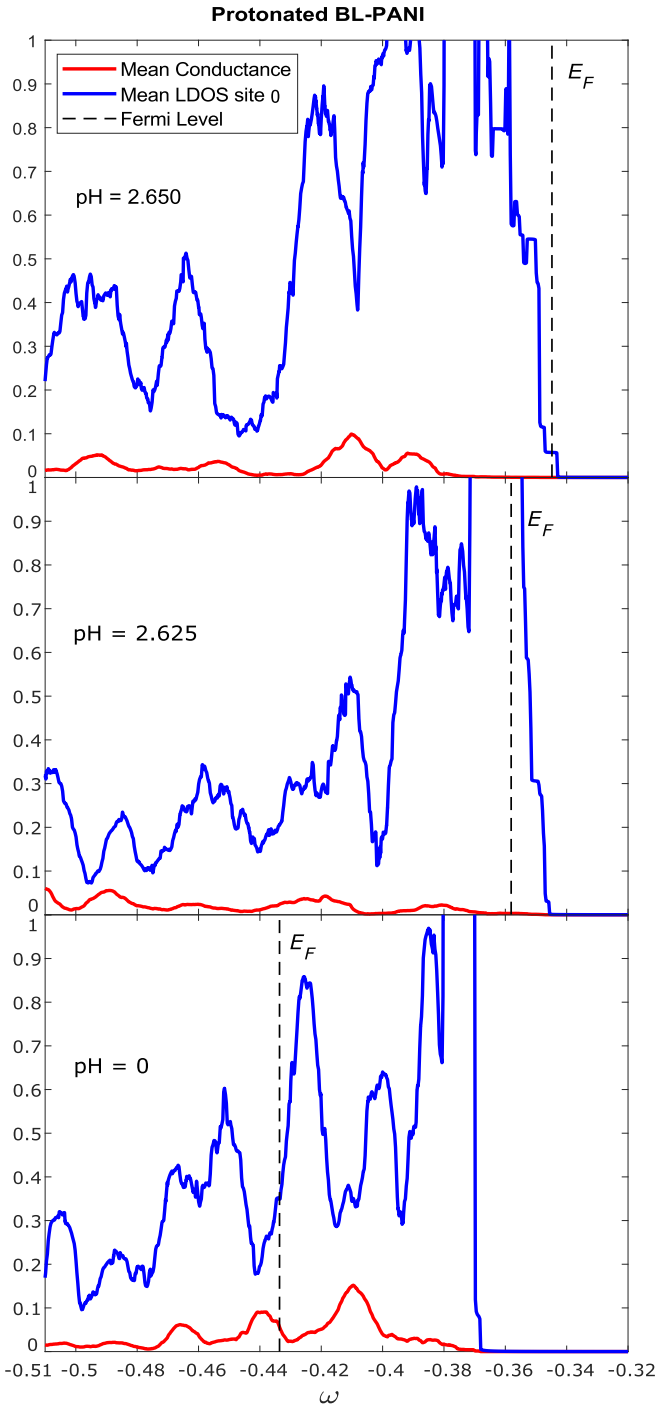

FIG. 7. Mean of the conductance and LDOS for a gradually protonated PANI at $\eta = 10^{-5}$, showing the respective Fermi level (dashed line).

in the deprotonated (P)/protonated (P^+) form. The effect of gradually doping BL-PANI is shown in Fig. 7 for $\eta = 10^{-5}$. We can observe the Fermi energy entering into the density of states region as the doping increases (pH decreases). For pH $\geqslant$ 2.625 and doping less than 5% (see Fig. 5), although the Fermi energy is located in the valence band region, it is within localized states above the mobility edge, as can be concluded by observing that the conductance is 0 at this energy, characterizing an insulator. For a larger value of doping, pH 0 in

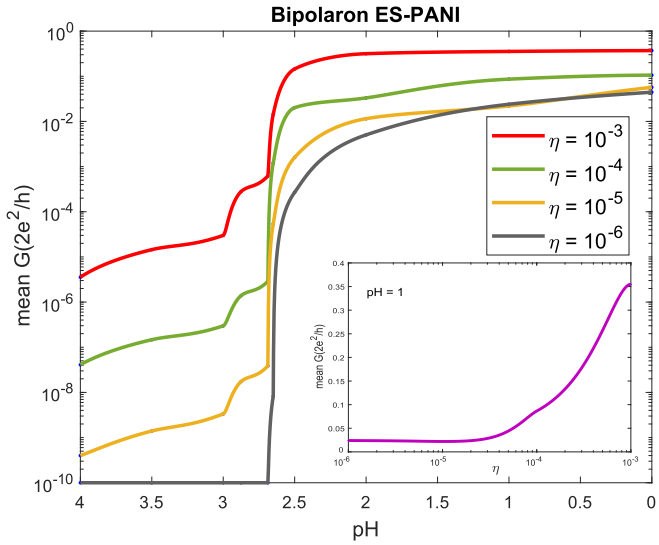

FIG. 8. Conductance behavior of a BL ES-PANI-like bipolaron as a function of the pH of the aqueous solution for various values of η. Inset: Behavior of the conductance as a function of the parameter η for pH 1.

Fig. 7, the Fermi energy is located below the mobility edge, in a region of delocalized states, characterizing the system as a metal.

These results show that it is critical, for a correct description of the metal-insulator transition, to be able to study in detail the electronic wave function phase interference that characterizes its localization and to determine the nature of the states at the Fermi level. As mentioned before, the calculation requires the regularization of the Green's function in the real axis introducing an imaginary part, η, in Eq. (2). This imaginary quantity gives rise to a spurious decoherence procedure that tends to destroy the spatial interference of the wave function that originates the localization. Consequently, to correctly describe the metal-nonmetal transition due to doping, it is necessary to study the problem in the limit of $\eta \to 0^+$.

The conductance is analyzed as a function of the rates of protonation. We study random BLs with extension $d = 6$, which gives a significant size in the conformation of the total system, $N > 1.4 \times 10^6$ sites, sufficient to generate good statistics in the calculations. In Fig. 8 we show the metal-insulator transition for the bipolaron ES-PANI lattice, by calculating the conductance in the protonation range $4 < \text{pH} < 0$ for various values of η decreasing to 0^+. This behavior was obtained taken the conductance as an average over 10^4 values of energy ω in an interval of $\Delta w = 10^{-3}$ around its respective Fermi level position, for each pH value. We observed that the conductance is accompanied by an abrupt increase between the values of pH 3 and pH 2.5, showing that the conductivity is strongly affected by the state of protonation (by doping) and undergoes a sharp metal-insulator transition. This result is consistent with many experimental results found in the literature in studies of the electrical properties of PANI [19,20,64–69], which report a rapid increase in conductivity in this pH region. It is evident that the dependence of the conductance on the parameter η is negligible for $\eta < 10^{-5}$, as can be

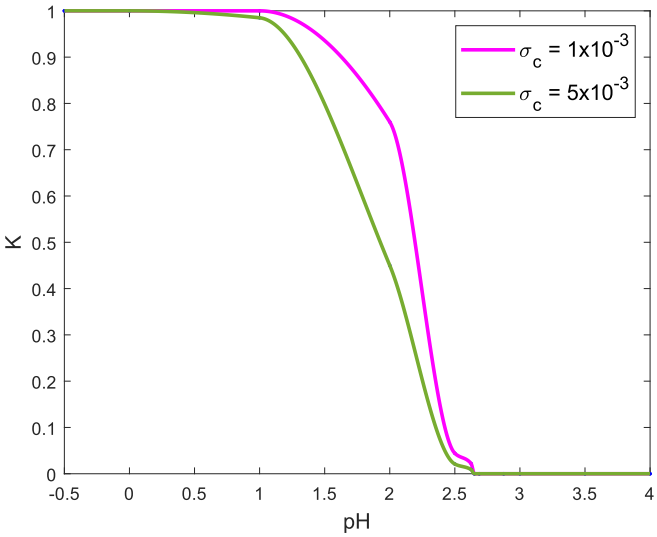

FIG. 9. The quantity K vs different concentrations of pH ($\eta = 10^{-6}$) for two values of σ_c.

concluded by inspection of the inset in Fig. 8,which has been arbitrarily taken for the case of pH 1.

For the purpose of producing extra validation of the metal-insulator transition observed in the pH-dependent conductance (Fig. 8), we apply the percolation threshold criterion [79], a formalism that provides a simple way of characterizing a metal-insulator transition in a disordered system. We define a parameter $K = NM/NT$, NT being the total number of states participating in the density of states in a small interval of energies $\Delta\omega = 10^{-3}$ and NM the number of states which contributes with a conductivity higher than an arbitrary small value in the same interval. According to this reasoning it would be possible to accurately determine the energy of the mobility edge by assuming that for values of ω in which $\sigma(w) < \sigma_c$ the state is localized.

We define two values for the conductance as the cutoff value σ_c (10^{-3} and 5×10^{-3}) in units of $2e^2/h$, which allows the establishment of a boundary between a conductor ($\sigma > \sigma_c$) and an insulator ($\sigma < \sigma_c$). We have considered the parameter K, calculated at each interval of $\Delta\omega = 10^{-3}$, as a mean result over 5×10^3 values of ω within the interval $\Delta\omega$ and the imaginary part of the energy $\eta = 10^{-6}$. Figure 9 shows the quantity K increasing for values higher than pH 2.625 and being qualitatively equivalent for the two values of σ_c taken to characterize the transition. This is in agreement with the behavior of the conductance as a function of the pH shown in Fig. 8.

The combination of Fig. 8 and Fig. 9 indicates that the model proposed to study doped polymerized PANI provides a realistic description of the metal-insulator transition, which accurately coincides with the experimental results [19,20,64–69].

V. CONCLUSIONS

A realistic treatment of the PANI lattice through a BL model was developed, considering the formation of disordered branched cross-linked chains and taking the phenazine molecule as a central structure to construct the ramified lattice. It was possible to study the charge transport properties of the nanostructure PANI, opening a new path to understand its electronic structure. This new approach overcomes the inadequate one-dimensional description [30], which gives rise to spatially localized states at the Fermi level for any doping and, consequently, is incapable of describing the metal-nonmetal transition that these systems go through when they are doped.

The adoption of phenazine as the fundamental nucleus in the cross-linking and growth of these branched lattices is compatible with many experimental studies reported in the literature [8,39–42,44,53], confirming its presence in the polymerization mechanism of PANI. The BL was modeled with coordinate number $Z = 4$, in correspondence with the branched PANI system. The lattice is constructed generating disordered linear chains of PANI in order to create a random BL cluster and using recursivity to build a final lattice with a large ($>10^6$) number of sites.

The electron transport properties were studied by calculating the LDOS and the conductance. The model assumed was able to describe the dramatic increase in the electrical conductivity observed in PANI under protonation. It was possible to corroborate the metal-insulator transition of the PANI at pH 2.625. The results obtained in this work established that the disorder and the concomitant Anderson localization in the conformation of these structures, due to doping and polymerization, play a fundamental role in explaining their conductivity properties.

The BL is a useful model to treat the cross-linked lattice formed in the oxidative polymerization of aniline and can serve as a reference point to study another polymer's systems. The possibility of building supramolecular structures with different morphologies such as films, nanowires, and nanotubes, considering these similar theoretical treatments, would open the possibility of studying the conductive characteristics and other electronic properties of these systems. These proposals will be the subject of an extension of this study in the future.

APPENDIX: DYSON'S EQUATIONS FOR THE BL-PANI MODEL

We can write the Green's function (GF) at site i of the BL system (Fig. 3), which is connected to the respective sites of the phenazine structure shown in Fig. 2, as

$$G_{ii}(w) = g_{ii} + g_{i\beta}t'G_{i'i} + g_{i\gamma}t'G_{i''i} + g_{i\delta}t'G_{i'''i}, \qquad \text{(A1)}$$

where g_{ii}, calculated by Eq. (2), is the undressed local diagonal GF in the main linear PANI connected to its phenazine and t' is the "hopping" term connecting the other linear PANIs with the phenazine's sites (subindexes β, γ, and δ as shown in Fig. 2). Here, in the initial stage, the respective nonlocal GFs, $G_{i'i}$, $G_{i''i}$, and $G_{i'''i}$, are given, respectively, by

$$G_{i'i}(w) = \tilde{g}_{i'}t'G_{\beta i}, \quad G_{i''i}(w) = \tilde{g}_{i''}t'G_{\gamma i},$$
$$G_{i'''i}(w) = \tilde{g}_{i'''}t'G_{\delta i}, \qquad \text{(A2)}$$

where $\tilde{g}_x$, $x = (i', i'', \text{and } i''')$, is obtained using Dyson's equation,

$$\tilde{g}_x(\varepsilon) = g_{xx} + \frac{\tilde{g}_0 t^2 g_{xj}^2}{1 - \tilde{g}_0 t^2 g_{jj}}, \qquad \text{(A3)}$$

where $\tilde{g}_0$ corresponds to the GF of the semi-infinite leads shown in Fig. 3, given by $\tilde{g}_0 = (w - i\sqrt{4t^2 - w^2})/2t^2$, and defined inside the band $-2t < w < 2t$.

The nonlocal dressed GFs between sites β, γ, and δ and site i are given by

$$\begin{aligned} G_{\beta i} &= g_{\beta i} + g_{\beta\beta}t' G_{i'i} + g_{\beta\gamma}t' G_{i''i} + g_{\beta\delta}t' G_{i'''i}, \\ G_{\gamma i} &= g_{\gamma i} + g_{\gamma\beta}t' G_{i'i} + g_{\gamma\gamma}t' G_{i''i} + g_{\gamma\delta}t' G_{i'''i}, \\ G_{\delta i} &= g_{\delta i} + g_{\delta\beta}t' G_{i'i} + g_{\delta\gamma}t' G_{i''i} + g_{\delta\delta}t' G_{i'''i}. \end{aligned} \tag{A4}$$

Based on the formulations of the GFs given above, we can form a system of equations that allows us to calculate the dressed GFs as

$$G_{i'i} = \frac{\begin{vmatrix} \tilde{g}_{i'}t' g_{\beta i} & -g_{\beta\gamma}t'^2\tilde{g}_{i'} & -g_{\beta\delta}t'^2\tilde{g}_{i'} \\ \tilde{g}_{i''}t' g_{\gamma i} & 1 - g_{\gamma\gamma}t'^2\tilde{g}_{i''} & -g_{\gamma\delta}t'^2\tilde{g}_{i''} \\ \tilde{g}_{i'''}t' g_{\delta i} & -g_{\delta\gamma}t'^2\tilde{g}_{i'''} & 1 - g_{\delta\delta}t'^2\tilde{g}_{i'''} \end{vmatrix}}{|\Delta|}, \tag{A5}$$

$$G_{i''i} = \frac{\begin{vmatrix} 1 - g_{\beta\beta}t'^2\tilde{g}_{i'} & \tilde{g}_{i'}t' g_{\beta i} & -g_{\beta\delta}t'^2\tilde{g}_{i'} \\ -g_{\gamma\beta}t'^2\tilde{g}_{i''} & \tilde{g}_{i''}t' g_{\gamma i} & -g_{\gamma\delta}t'^2\tilde{g}_{i''} \\ -g_{\delta\beta}t'^2\tilde{g}_{i'''} & \tilde{g}_{i'''}t' g_{\delta i} & 1 - g_{\delta\delta}t'^2\tilde{g}_{i'''} \end{vmatrix}}{|\Delta|}, \tag{A6}$$

$$G_{i'''i} = \frac{\begin{vmatrix} 1 - g_{\beta\beta}t'^2\tilde{g}_{i'} & -g_{\beta\gamma}t'^2\tilde{g}_{i'} & \tilde{g}_{i'}t' g_{\beta i} \\ -g_{\gamma\beta}t'^2\tilde{g}_{i''} & 1 - g_{\gamma\gamma}t'^2\tilde{g}_{i''} & \tilde{g}_{i''}t' g_{\gamma i} \\ -g_{\delta\beta}t'^2\tilde{g}_{i'''} & -g_{\delta\gamma}t'^2\tilde{g}_{i'''} & \tilde{g}_{i'''}t' g_{\delta i} \end{vmatrix}}{|\Delta|}; \tag{A7}$$

here Δ is the determinant of the matrix of coefficients of the system of equations

$$\Delta = \begin{vmatrix} 1 - g_{\beta\beta}t'^2\tilde{g}_{i'} & -g_{\beta\gamma}t'^2\tilde{g}_{i'} & -g_{\beta\delta}t'^2\tilde{g}_{i'} \\ -g_{\gamma\beta}t'^2\tilde{g}_{i''} & 1 - g_{\gamma\gamma}t'^2\tilde{g}_{i''} & -g_{\gamma\delta}t'^2\tilde{g}_{i''} \\ -g_{\delta\beta}t'^2\tilde{g}_{i'''} & -g_{\delta\gamma}t'^2\tilde{g}_{i'''} & 1 - g_{\delta\delta}t'^2\tilde{g}_{i'''} \end{vmatrix}. \tag{A8}$$

Finally, substituting the dressed GF into Eqs. (A4), (A2), and (A1), we get G_{ii} in the first BL-PANI. It is evident that this way of building a BL-PANI represents an exact recursive procedure for generating a large extensive BL-PANI in the final stage. This procedure avoids the diagonalization of a large matrix representing the complete lattice and permits working with a much larger system.

[1] D. Y. Liu and J. R. Reynolds, ACS Appl. Mater. Interfaces **2**, 3586 (2010).
[2] J. Jang, J. Bae, M. Choi, and S.-H. Yoon, Carbon **43**, 2730 (2005).
[3] N. S. Azar and M. Pourfath, IEEE Trans. Electron Devices **62**, 1584 (2015).
[4] R. Ramya, R. Sivasubramanian, and M. Sangaranarayanan, Electrochim. Acta **101**, 109 (2013).
[5] F. Zhang, M. Johansson, M. Andersson, J. Hummelen, and O. Inganäs, Adv. Mater. **14**, 662 (2002).
[6] G. Ćirić-Marjanović, M. Trchová, and J. Stejskal, Collect. Czech. Chem. Commun. **71**, 1407 (2006).
[7] G. Ćirić-Marjanović, E. N. Konyushenko, M. Trchová, and J. Stejskal, Synth. Met. **158**, 200 (2008).
[8] G. Ćirić-Marjanović, M. Trchová, and J. Stejskal, Int. J. Quantum Chem. **108**, 318 (2008).
[9] N. Gospodinova and L. Terlemezyan, Prog. Polym. Sci. **23**, 1443 (1998).
[10] N. Gospodinova, L. Terlemezyan, P. Mokreva, and K. Kossev, Polymer **34**, 2434 (1993).
[11] Y. Ding, A. Buyle Padias, and H. K. Hall, J. Polym. Sci. Part A: Polym. Chem. **37**, 2569 (1999).
[12] R. Madathil, S. Ponrathnam, and H. Byrne, Polymer **45**, 5465 (2004).
[13] S. P. Surwade, V. Dua, N. Manohar, S. K. Manohar, E. Beck, and J. P. Ferraris, Synth. Met. **159**, 445 (2009).
[14] E. C. Venancio, P.-C. Wang, and A. MacDiarmid, Synth. Met. **156**, 357 (2006).
[15] D. C. Ferreira, J. R. Pires, and M. L. A. Temperini, J. Phys. Chem. B **115**, 1368 (2011).
[16] H. D. Tran, J. M. D'Arcy, Y. Wang, P. J. Beltramo, V. A. Strong, and R. B. Kaner, J. Mater. Chem. **21**, 3534 (2011).
[17] J. Stejskal, I. Sapurina, and M. Trchová, Prog. Polym. Sci. **35**, 1420 (2010).
[18] I. Sapurina and J. Stejskal, Polym. Int. **57**, 1295 (2008).
[19] A. Epstein, J. Ginder, F. Zuo, H.-S. Woo, D. Tanner, A. Richter, M. Angelopoulos, W.-S. Huang, and A. MacDiarmid, Synth. Met. **21**, 63 (1987).
[20] A. Macdiarmid, J. Chiang, A. Richter, and A. Epstein, Synth. Met. **18**, 285 (1987).
[21] D. S. Galvão, D. A. dos Santos, B. Laks, C. P. de Melo, and M. J. Caldas, Phys. Rev. Lett. **63**, 786 (1989).
[22] H.-L. Wu and P. Phillips, Phys. Rev. Lett. **66**, 1366 (1991).
[23] A. Varela-Álvarez, J. A. Sordo, and G. E. Scuseria, J. Am. Chem. Soc. **127**, 11318 (2005).
[24] C. J. Cattena, R. A. Bustos-Marún, and H. M. Pastawski, Phys. Rev. B **82**, 144201 (2010).
[25] F. C. Lavarda, M. C. dos Santos, D. S. Galvão, and B. Laks, Phys. Rev. Lett. **73**, 1267 (1994).
[26] J. L. D'Amato and H. M. Pastawski, Phys. Rev. B **41**, 7411 (1990).
[27] A. Varela-Álvarez and J. A. Sordo, J. Chem. Phys. **128**, 174706 (2008).
[28] R. Farchioni, P. Vignolo, and G. Grosso, Phys. Rev. B **60**, 15705 (1999).
[29] R. Farchioni, G. Grosso, and G. P. Parravicini, Phys. Rev. B **53**, 4294 (1996).
[30] R. A. Padilla, M. A. Pacheco, and E. V. Anda, Mater. Res. Express **5**, 065312 (2018).
[31] P. W. Anderson, Phys. Rev. **109**, 1492 (1958).
[32] J. Joo, Z. Oblakowski, G. Du, J. P. Pouget, E. J. Oh, J. M. Wiesinger, Y. Min, A. G. MacDiarmid, and A. J. Epstein, Phys. Rev. B **49**, 2977 (1994).
[33] Z. H. Wang, H. H. S. Javadi, A. Ray, A. G. MacDiarmid, and A. J. Epstein, Phys. Rev. B **42**, 5411 (1990).
[34] J. Joo, V. N. Prigodin, Y. G. Min, A. G. MacDiarmid, and A. J. Epstein, Phys. Rev. B **50**, 12226 (1994).

[35] M. I. Salkola and S. A. Kivelson, Phys. Rev. B **50**, 13962 (1994).
[36] V. N. Prigodin and K. B. Efetov, Phys. Rev. Lett. **70**, 2932 (1993).
[37] C. Laslau, Z. Zujovic, and J. Travas-Sejdic, Prog. Polym. Sci. **35**, 1403 (2010).
[38] A. N. Ivanova, A. V. Tadjer, and N. P. Gospodinova, J. Phys. Chem. B **110**, 2555 (2006).
[39] A. Kellenberger, E. Dmitrieva, and L. Dunsch, Phys. Chem. Chem. Phys. **13**, 3411 (2011).
[40] Y.-W. Cheng, L. Chao, Y.-M. Wang, K.-S. Ho, S.-Y. Shen, T.-H. Hsieh, and Y.-Z. Wang, Synth. Met. **168**, 48 (2013).
[41] E. Dmitrieva, Y. Harima, and L. Dunsch, J. Phys. Chem. B **113**, 16131 (2009).
[42] G. Inzelt and Z. Puskás, Electrochim. Acta **49**, 1969 (2004).
[43] B. Sarma, L. S. Reddy, and A. Nangia, Cryst. Growth Des. **8**, 4546 (2008).
[44] G. Ćirić-Marjanović, M. Trchová, and J. Stejskal, J. Raman Spectrosc. **39**, 1375 (2008).
[45] S. Bhadra and D. Khastgir, Polym. Degrad. Stab. **93**, 1094 (2008).
[46] J. A. Conklin, S.-C. Huang, S.-M. Huang, T. Wen, and R. B. Kaner, Macromolecules **28**, 6522 (1995).
[47] L. Ding, X. Wang, and R. Gregory, Synth. Met. **104**, 73 (1999).
[48] Y. Wei, G.-W. Jang, K. F. Hsueh, E. M. Scherr, A. G. MacDiarmid, and A. J. Epstein, Polymer **33**, 314 (1992).
[49] K. Luo, N. Shi, and C. Sun, Polym. Degrad. Stab. **91**, 2660 (2006).
[50] R. Mathew, B. R. Mattes, and M. P. Espe, Synth. Met. **131**, 141 (2002).
[51] G. M. D. Nascimento, C. H. Silva, and M. L. Temperini, Polym. Degrad. Stab. **93**, 291 (2008).
[52] H. H. Tan, K. G. Neoh, F. T. Liu, N. Kocherginsky, and E. T. Kang, J. Appl. Polym. Sci. **80**, 1 (2001).
[53] Z. Ding, T. Sanchez, A. Labouriau, S. Iyer, T. Larson, R. Currier, Y. Zhao, and D. Yang, J. Phys. Chem. B **114**, 10337 (2010).
[54] Y. Shimoi and S. Abe, Phys. Rev. B **50**, 14781 (1994).
[55] J. Tang, R. D. Allendoerfer, and R. A. Osteryoung, J. Phys. Chem. **96**, 3531 (1992).
[56] M. E. Jozefowicz, R. Laversanne, H. H. S. Javadi, A. J. Epstein, J. P. Pouget, X. Tang, and A. G. MacDiarmid, Phys. Rev. B **39**, 12958 (1989).
[57] M. Nechtschein, F. Genoud, C. Menardo, K. Mizoguchi, J. Travers, and B. Villeret, Synth. Met. **29**, 211 (1989).
[58] F. Zuo, M. Angelopoulos, A. G. MacDiarmid, and A. J. Epstein, Phys. Rev. B **39**, 3570 (1989).
[59] P. Vignolo, R. Farchioni, and G. Grosso, Phys. Status Solidi (b) **223**, 853 (2001).
[60] A. Streitwieser, *Molecular Orbital Theory* (Wiley, New York, 1961).
[61] L. P. Kadanoff and G. B. Benjamin, *Quantum Statistical Mechanics* (W. A. Benjamin, New York, 1962).
[62] L. V. Keldysh, Zh. Eksp. Teor. Fiz. **47**, 1515 (1964) [Sov. Phys. JETP **20**, 1018 (1965)].
[63] R. Landauer and M. Büttiker, Phys. Rev. Lett. **54**, 2049 (1985).
[64] H. Pingsheng, Q. Xiaohua, and L. Chune, Synth. Met. **57**, 5008 (1993).
[65] J. Stejskal and R. G. Gilbert, Pure Appl. Chem. **74**, 857 (2002).
[66] N. V. Blinova, J. Stejskal, M. Trchová, and J. Prokeš, Polym. Int. **57**, 66 (2009).
[67] R. Singh, V. Arora, R. Tandon, S. Chandra, N. Kumar, and A. Mansingh, Polymer **38**, 4897 (1997).
[68] V. Luthra, R. Singh, S. Gupta, and A. Mansingh, Curr. Appl. Phys. **3**, 219 (2003).
[69] S. Kumar Gupta, V. Luthra, and R. Singh, Bull. Mater. Sci. **35**, 787 (2012).
[70] D. Weaire and M. F. Thorpe, Phys. Rev. B **4**, 2508 (1971).
[71] M. F. Thorpe and D. Weaire, Phys. Rev. B **4**, 3518 (1971).
[72] M. F. Thorpe, D. Weaire, and R. Alben, Phys. Rev. B **7**, 3777 (1973).
[73] J. d'Albuquerque e Castro, J. Phys. C: Solid State Phys. **17**, 5945 (1984).
[74] M. R. Zirnbauer, Phys. Rev. B **34**, 6394 (1986).
[75] R. Abou-Chacra, D. J. Thouless, and P. W. Anderson, J. Phys. C: Solid State Phys. **6**, 1734 (1973).
[76] R. Abou-Chacra and D. J. Thouless, J. Phys. C: Solid State Phys. **7**, 65 (1974).
[77] A. D. Mirlin and Y. V. Fyodorov, Nucl. Phys. B **366**, 507 (1991).
[78] A. D. Mirlin and Y. V. Fyodorov, Phys. Rev. Lett. **72**, 526 (1994).
[79] A. Latgé and E. Anda, Solid State Commun. **76**, 1387 (1990).
[80] D. N. Zubarev, Sov. Phys. Uspekhi **3**, 320 (1960).
[81] R. Kubo, J. Phys. Soc. Jpn. **12**, 570 (1957).
[82] H. Reiss, J. Phys. Chem. **92**, 3657 (1988).
[83] H. Reiss, Synth. Met. **30**, 257 (1989).
[84] X. Chen, C. A. Yuan, C. K. Wong, H. Ye, S. Y. Leung, and G. Zhang, Sensors Actuat. B: Chem. **174**, 210 (2012).